JET-P(94)09

Overview of High Performance H-modes in JET

The JET Team
presented by D Stork.

JET Joint Undertaking, Abingdon, Oxon, OX14 3EA, UK.

Preprint of a paper to be Submitted for publication in
Plasma Physics and Controlled Fusion
(Proceedings of 4th IAEA TCM on H-mode Physics)

February 1994

ABSTRACT

An account is given of the high performance plasmas established by development of the H-mode regime in JET in the experimental campaigns up to 1992. High performance in this case is measured in terms of the confinement enhancement achieved over the L-mode scaling as measured using the plasma diamagnetism. Three JET H-mode regimes have achieved enhancement factors (H_G^{DIA}) over Goldston L-mode scaling of $2.5 < H_G^{DIA} < 4.0$. These are the Pellet Enhanced Performance (PEP) H-mode, the high bootstrap fraction (high β_{POL}) H-mode and the Hot Ion (HI) H-mode. The phenomenology of these three regimes is reviewed and contrasts and common threads are elucidated. All the regimes are transient (on a resistive diffusion timescale) and the mechanisms terminating the period of enhanced confinement are discussed. Common features between the high β_{POL} and HI regimes are identified which suggest that they are effectively two aspects of a unified Very High (VH) confinement regime. The experimental conditions for accessing this regime are reviewed.

1. INTRODUCTION

The JET device has carried out many experiments on H-mode plasmas between the establishment of the first such discharges in JET (Tanga et al, 1987) and the major shutdown of JET, which was started in February 1992, in order to install the Pumped Divertor. This series of experiments saw successful plasmas of the ELMy H-mode type; ELM free H-modes and three H-mode regimes with elevated confinement. These three regimes were the Pellet Enhanced Plasma (PEP) H-mode; the Bootstrap dominated or high β_{POL} H-mode and the Hot Ion (HI) H-mode.

The development of ELMy H-modes is reviewed in these proceeding by Campbell et al. Such H-modes have been obtained in quasi steady state conditions (with respect to energy and particle confinement times τ_E and τ_p). The other JET H-mode regimes are all significantly more transient in nature.

The important characteristic times for a fusion plasma are the energy confinement time (τ_E); particle confinement time (τ_p); resistive diffusion time ($\tau_R = 4\pi L_c^2/\eta_{neo}\,(Z_{eff}, T_e)\cdot c^2$, where L_c is a characteristic length usually taken as the plasma minor radius, η_{neo} is the neoclassical resistivity, T_e the plasma electron temperature and Z_{eff} the effective ion charge); wall residence time (τ_w);

the wall pumping saturation time (τ_{wps}), and the active pumping time (if any). For steady density, temperature and MHD stability profiles one would ideally require the duration of a regime (t_d) to satisfy:

$$t_d > 3\tau_E \qquad t_d > 3\tau_p \qquad t_d > 3\tau_R$$

whilst for hydrogenic recycling evolution to reach steady state $t_d > 3\tau_W$ would be required.

At high power (> 15MW), the JET H-mode regime is transitory with respect to all of the above criteria. The record stored energy in a JET H-mode (12.7MJ in a Double Null X-point (DNX) configuration obtained with 22MW of additional heating) was achieved in an H-mode phase lasting less than 1 second (Jones et al, 1992). Although the phase lasted for around 1.5 energy confinement times, its duration was less than 50% of the particle confinement time and only around 1-2% of the resistive diffusion time. At high powers, these JET ELM-free H-modes are degraded by severe impurity influx following a carbon or beryllium bloom from the X-point tiles (Stork et al, 1991). At medium powers (~ 7-8MW), the H-mode regime has been sustained for long enough to be terminated by the onset of 100% power radiation. This is caused by the rising density in Neutral Beam Injection (NBI) heated H-modes, there being no method of pumping the ~ 10^{21} particles sec^{-1} influx in these JET discharges. These longer H-modes, lasting for around $7 \times \tau_E$ or $1\text{-}2 \times \tau_P$, can be achieved with control of impurities using strong gas puffing (Stork et al, 1990). The poor performance with respect to active density control in previous JET plasmas should be improved when the new JET pumped divertor comes into operation (Rebut, 1990). At present, apart from the ELMy H-modes, there has only been occasional evidence of density control in JET H-modes heated by Ion Cyclotron Radio Frequency (ICRF) heating alone: the so-called Low Particle Confinement (LPC) H-mode which achieves confinement enhancement close to twice the Goldston L-mode value with a constant density (Bhatnagar et al, 1991).

The JET ELM-free H-modes described above have confinement enhancements with respect to Goldston L-mode scaling (H_G^{DIA}) of 2-2.2. However, there exist several H-mode regimes in which it is possible to substantially improve the confinement. These 'elevated' confinement regimes are defined such that the enhancement factor H_G^{DIA} is > 2.5 or alternatively, that the enhancement of thermal stored energy is significant relative to the JET/DIIID H-mode scaling (Schissel et al, 1991).

Defining $H^{th}_{J/DIII} = \tau^{th}_E / \tau_{E,J/DIII}$ where $\tau_{E,J/DIII} = 0.106\ P_L^{-0.46}\ I_p^{1.03}\ R^{1.48}$ (MW, MA, m) the elevated confinement regimes have $H^{th}_{J/DIII} > 1.25$. Typical confinement values in the three discharges types (the PEP H-mode, high β_{POL} H-mode and HI H-mode) are shown in fig. 1. These discharges form the subject matter of this paper. Section 2 covers the phenomenology of confinement and termination in the PEP H-mode; section 3 review the high β_{POL} H-mode and section 4 the Hot Ion (HI) H-modes. The common characteristics of the high β_{POL} and HI regimes are reviewed in section 5 where a common Very High confinement (VH) regime is proposed. Section 6 explores the experimental conditions for accessing the VH regime. More details about the confinement systematics in the JET VH regime can be found in the paper of Thomsen et al, in these proceedings.

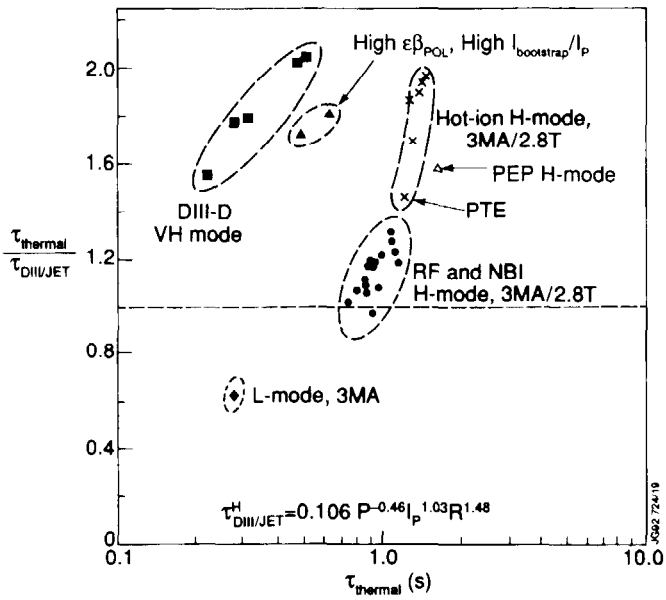

Fig.1. Thermal energy confinement times for JET Hot Ion H-modes and other JET 3MA H-modes normalised to the DIII-D/JET H-mode scaling. Also shown are JET H-modes with high bootstrap current ($I_{boot}/I_p \sim 0.7$) at 1-1.5MA and the 3MA PEP H-mode. The First Tritium Experiment shot is labelled 'PTE'.

2. THE PEP H-MODE REGIME

The Pellet Enhancement Plasma (PEP) phenomenon features a dense plasma core ($r/a < 0.3$-0.4) created by the injection of 4-6mm pellets followed by the application of strong additional heating. The peaked density profiles of the PEP have been combined with the edge related confinement enhancement obtained in the H-mode regime (Tubbing et al, 1991).

The pellet injection takes place prior to the onset of sawteeth before the $q = 1$ surface has entered the plasma. Immediately after the pellet injection, strong additional heating is applied and the PEP H-mode has been obtained with NBI heating, ICRF heating and combined heating schemes. The duration of the PEP H-mode phase is typically 0.5-1.0 seconds, which is around 50-100% of the energy confinement time but only ~ 3% of the resistive diffusion time in the core. The

PEP H-modes have been developed using up to 28MW of additional power, but the highest fusion performance (~ 2.10^{16} neutrons sec^{-1}) has been obtained using approximately 11MW of NBI heating with a small amount of ICRF (Bures et al, 1993). The central power deposition of the ICRF was essential to achieve the highest performance. Some of these discharges have global confinement enhancement (H_G^{DIA}) values of around 3.

2.1 Confinement in the PEP H-mode regime

The PEP confinement properties can be seen by comparing an H-mode with a PEP H-mode under similar conditions (Balet et al, 1993). Fig. 2(a) shows the time evolution of two almost identical NBI heated discharges, one with a 4mm pellet injected at 5 seconds and the other without. In the case where the pellet is used, higher values are obtained for the plasma stored energy and neutron yield. In fig. 2(b), the effect of the PEP is evidenced by a significantly higher central electron density. Fig. 3 shows the effective heat conductivity profiles for the two pulses. The central region of enhanced confinement can be clearly seen.

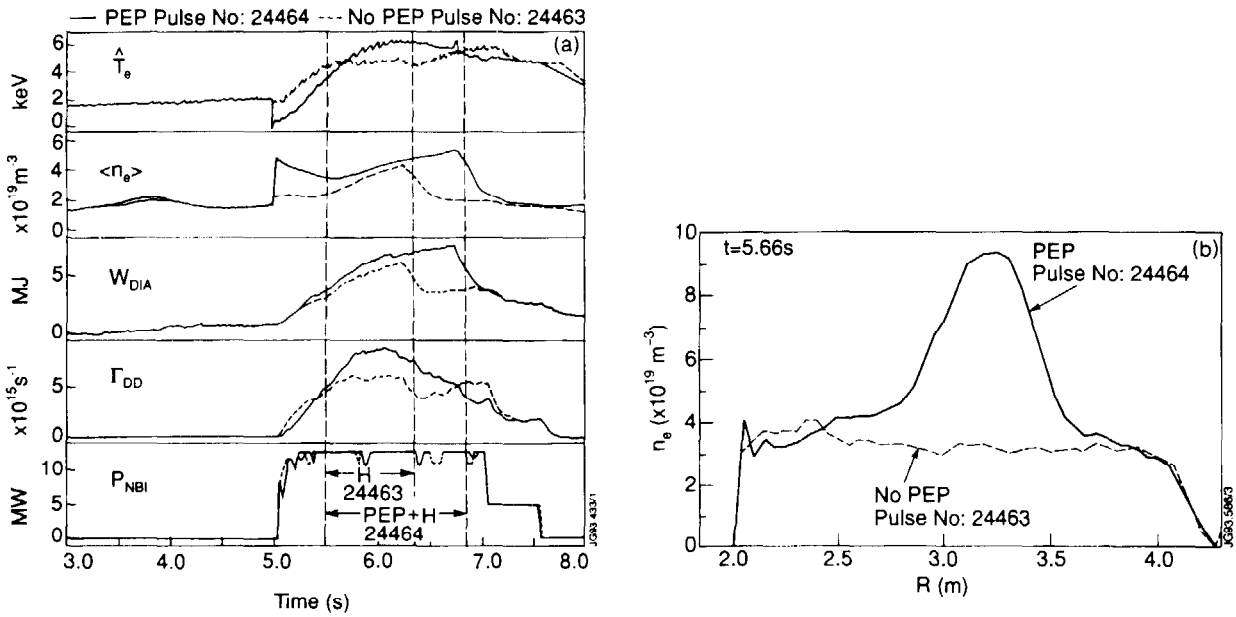

Fig.2 (a). Comparison of the time evolution of the central electron temperature, volume-averaged plasma diamagnetic energy, total neutron rate and NBI power of an NBI-heated H-mode with (pulse 24464) and without (pulse 24463) the PEP density enhancement.

(b). Plasma electron density profile measured at t = 5.66s using the LIDAR Thomson scattering diagnostic for the two pulses in (a).

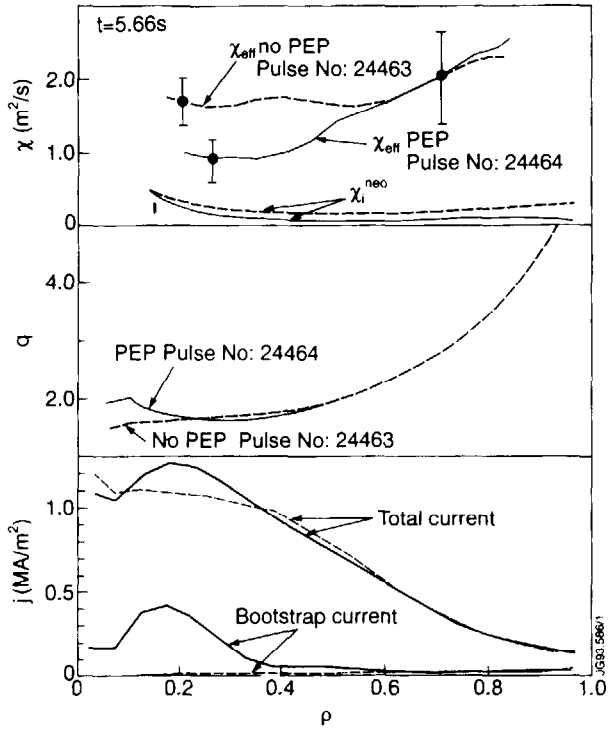

Fig.3. For the pulses shown in fig. 2;

- calculated heat conductivity χ_{eff} versus normalised radius ρ (upper graph);
  calculated safety factor profile versus ρ (middle graph);
  calculated total current and bootstrap current profiles versus ρ (lower graph).

Fig. 3 also shows the non-inductive current density profiles calculated using TRANSP for these two pulses. In the PEP discharge, the bootstrap current dominates due to the steep pressure gradient near to the plasma centre. In thecase without the PEP, the beam driven current dominates due to lower central density and results in a centrally peaked non-inductive current profile. The resulting q profile calculated using TRANSP is also shown in Fig. 3. The effect of pellet injection combined with the off-axis bootstrap current is to produce a region of negative shear in the plasma core. Current profile measurements made using the polarimeter and observations of MHD activity on other PEP discharges, are supportive of this conclusion. The negative shear may play a role in the enhancement of the local confinement. A prediction to this effect comes from the Rebut-Lallia-Watkins local transport model (Rebut et al, 1988). Note however that the region of improved confinement is somewhat larger than the negative shear region. The particle diffusion in the core of the PEP H-mode also appears to be reduced below the normal L mode values, effective particle diffusion coefficients (D_{eff}) ~ $0.1 m^2 s^{-1}$ being achieved.

The relatively small volume of reduced transport leaves variable impact on global H_G^{DIA}, and correlations of H_G^{DIA} and χ_{eff}(core) with plasma parameters such as ∇n, ∇T, $\nabla n/n$, and $\nabla T/T$ reveal no systematic variation. The reason for

this is that ELM activity and Z_{eff} profiles also vary across the PEP H-mode dataset. These variations obscure correlations with the core parameters.

Central heating, by the deposition of RF power within $r/a < 0.4$ leads to an improvement in the central parameters of the discharge (T_i, T_e) and also to the fusion performance. How-ever the value of χ_{eff} remains the same in the plasma core (Balet et al, 1993), and no synergistic effects are required to explain the improvement in parameters. At the central densities achieved in the best PEPs ($\geq 8.10^{19}m^{-3}$), equipartition ensures that $T_i \sim T_e$. In these cases the highest ion temperatures achieved on JET with ICRF heating ($T_i(0) \sim 14.5keV$) have been measured.

2.2 Termination of the PEP H-mode

The termination phase of the PEP H-mode exhibits a wide variety of phenomenology. JET MHD diagnostics have been restricted to the detection of $n \leq 4$ modes and have had limited fast sampling capability. Hence it is possible that MHD activity, especially the high-n activity associated with ballooning modes, may have escaped detection. With this caveat we find that less than 50% of the JET PEP discharges have *identifiable* MHD collapses. In about 25% of the cases, $n = 1$ activity is associated with the collapse of the central parameters (identified as the rapid decline in the measured DD fusion reaction rate) whilst about 10% show $n = 3$ activity followed by $n = 1$ activity. Some MHD collapses can be seen to be directly responsible for impurity accumulation in the core which leads to the PEP phase collapse. The reasons for the variable MHD activity have their origins in the variation of q profile after the pellet injection. As indicated in Fig. 2, the PEP q profile features an off-axis minimum. The value of q_o and q_{min} post-pellet varies from discharge to discharge. As the heating is applied, the evolving bootstrap current drives q_o up and q_{min} down. Simulations with the FAR code shows that the sequence of distabilisation of $n = 3$ or $n = 2$ or $n = 1$ resistive kinks depends on the initial values of q_o and q_{min} (Smeulders et al, 1993), hence providing an explanation for the differences in low n activity which are seen.

Regarding ballooning stability of the PEP H-modes, the comparison of code simulations with measured pressure profiles show that the core of the PEP plasmas are in the region of so-called second stability against Ideal Ballooning modes. This access to second stability is opened up by two factors:

i) the minimum q in the PEP H-modes is ≥ 1.2 in most cases which joins the first and second stable regions for a plasma with low positive shear; and

ii) the region of negative shear exists without a first stable boundary and, if the shear is sufficiently negative, is also free of the Mercier instability.

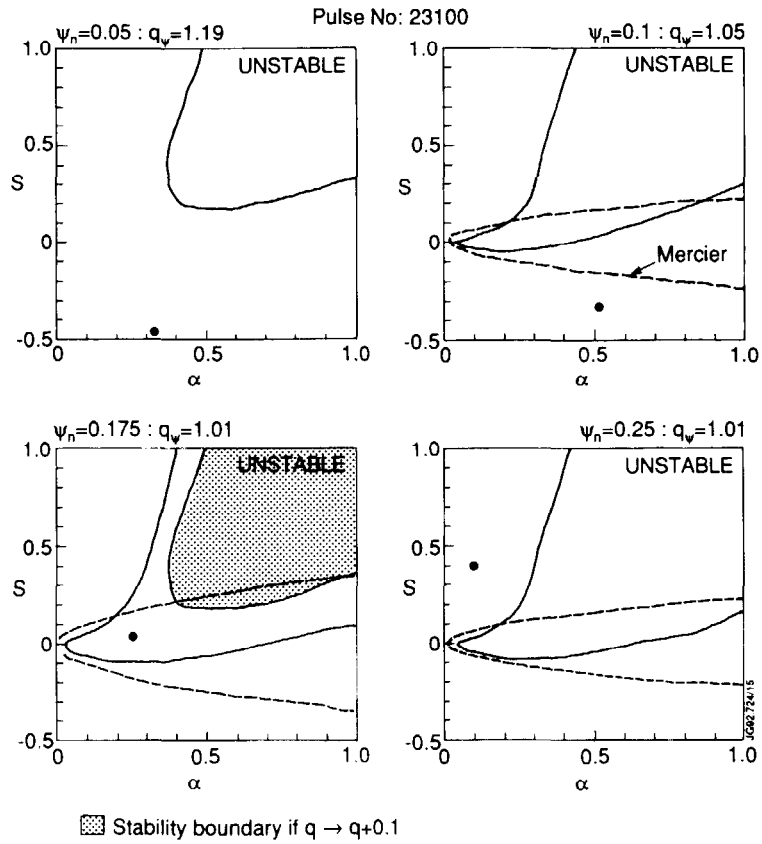

Fig.4. Ideal ballooning s-α analysis for central flux surfaces of a PEP+H mode just prior to the decline in the fusion reaction rate. The bottom left graph indicates the change in the unstable region if the measured safety factor (q) is replaced by q + 0.1.

As the current profile evolves in the PEP phase and q_{min} drops below ~ 1.1, the second stable region is cut off and analyses suggest that either ballooning or Mercier modes may become unstable and cause the collapse of the PEP phase. A s-α diagram analysis for a typical PEP shot is shown in fig. 4. The uncertainties in the position of the stability boundary are quite significant due to uncertainties in the q profile (which are at least $\Delta q \sim \pm 0.1$) and hence a definitive statement cannot be made on this point.

3. HIGH β_{POL} H-MODE REGIME

In the JET high β_{POL} H-mode study (Challis et al, 1993) the aim was to produce H-modes with a high fraction of the current sustained by the bootstrap mechanism in reactor relevant conditions ($I_{boot}/I_p > 60\%$). These conditions were defined by having negligible central particle fuelling and flat density profiles with gas fuelling. In order to ensure negligible central particle fuelling, the experiments were performed using ICRF heated, double null X-point plasmas with I_P = 1-1.5MA and B_T = 2.8-3.1T. Strong gas puffing was required to maintain the ICRF coupling at reasonable power levels.

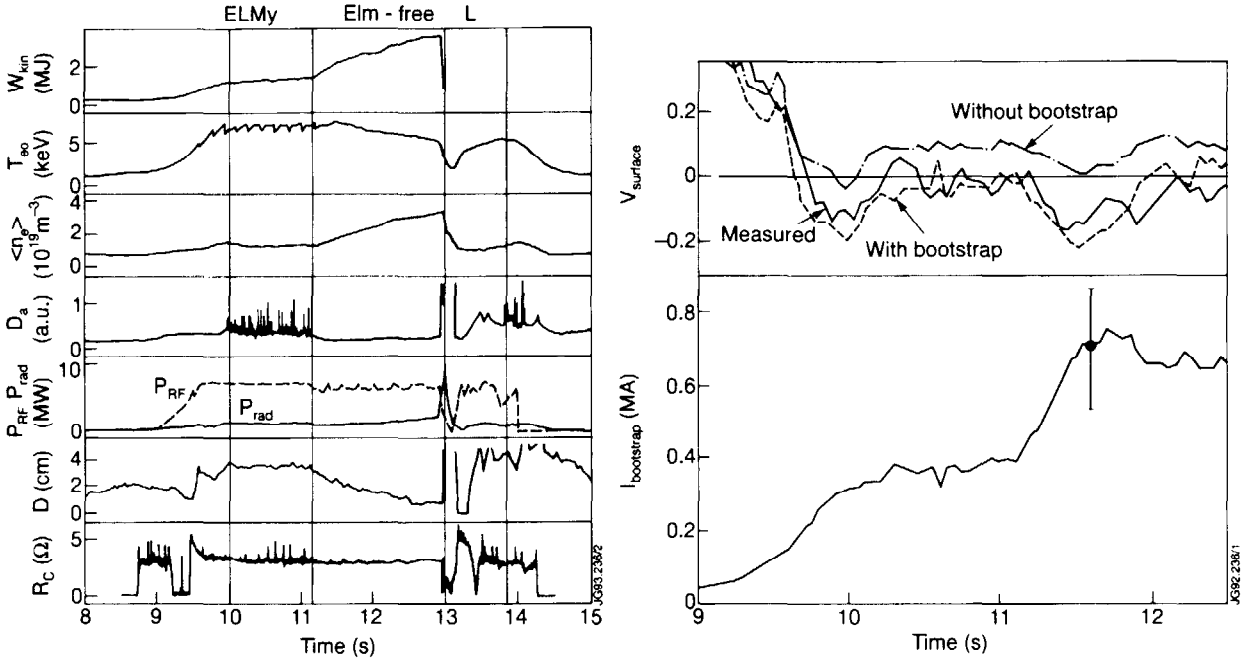

Fig.5(a). Evolution of parameters in a 1MA ICRF heated H-mode. The antenna-plasma distance (D, sixth trace from top) becomes progressively smaller as the H mode evolves and the feedback system moves the plasma to keep the coupling (bottom trace) constant;
(b). Surface loop voltage against time compared to TRANSP simulations with and without the bootstrap current term shown in the second graph for the 1MA pulse #25264.

Fig. 5(a) shows the time evolution of a typical (1MA/2.8T) discharge. ELMs are observed soon after the application of the heating and this maintains constant density for more than 1s. The discharge then makes a transition into an

ELM free H-mode and the sawteeth terminate. The density and thermal plasma energy rises strongly until $\beta_{POL} \sim 2$ is reached. The ELM free phase is usually

terminated by an event associated with a giant ELM resulting in a loss of more than half the electron density and plasma energy.

3.1 Bootstrap analysis

A time dependent analysis of the JET high β_{POL} discharges using the TRANSP code has calculated the current profile evolution. The simulation which includes neoclassical resistivity and the bootstrap current, uses the measured temperature and density profiles. Suprathermal ion pressure, expected to be small in the high density phase, is excluded from the analysis. Fig. 5(b) shows the TRANSP calculation compared to the measured loop voltage. The sign reversal of the loop voltage is only reproduced when the bootstrap effect is included. In the ELM-free phase the bootstrap current rises to dominate the total plasma current ($I_b/I_p \sim 0.7 \pm 0.15$).

An analysis of the current profile evolution (Challis et al, 1993) shows that the bootstrap current is located at large radii. The duration of these high β_{POL} H-modes is long compared with the characteristic energy confinement time ($t_d \sim 4\tau_E$) but very short compared to the characteristic resistive diffusion time ($t_d \sim 0.04\tau_R$). The current distribution is thus far from the steady state profile which would result in an axial $q_o \sim 3$ to be expected with a 70% bootstrap fraction.

3.2 Confinement in the high β_{POL} H-modes

The thermal energy confinement time (τ_E^{th}) is enhanced beyond the normal H-mode, being up to 70% better than the value given by the DIIID-JET H-mode scaling. The local transport analysis with the TRANSP code shows that the confinement improvement occurs throughout the volume of the plasma.

Fig. 6 shows a comparison of χ_{eff} for the high β_{POL} ELM free H-mode phase and an extrapolation of a 'normal' 3MA ICRF-only H-mode (Balet et al, 1991). The two H-modes have very similar applied ICRF power and electron temperature profiles. A simple scaling of τ_E with plasma current as $I_p^{1.0}$ does not fit the data when applied between the two plasmas (this is done locally by scaling χ_{eff} by $1/B_{POL}$ in going from 3MA to 1MA). A scaling of χ_{eff} with local shear, as $s^{-\gamma}$ would require $|\gamma| >> 1$ contrary to experience from local transport results in JET current ramp experiments (Challis et al, 1992) which gave $\chi_{eff} \sim s^{-\gamma}$ with $0 < |\gamma| < 1$.

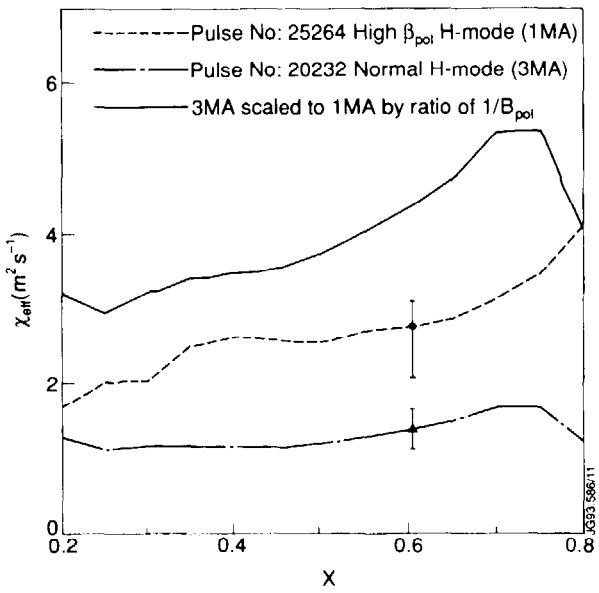

Fig.6. Radial profiles of effective thermal diffusivity (χ_{eff}) obtained from TRANSP analyses of the 1MA/2.8T high β_{POL} H-mode pulse #25264 (small dashes) and the 3MA/2.8T ICRF heated H-mode discharge pulse #20232 (dot-dash). The 3MA data scaled to 1MA using (χ_{eff}) (scaled) = χ_{eff} (3MA)*(B_{POL} (3MA/B_{POL} (1MA)) is also shown (dashed lines). Error bars show the typical range of χ_{eff} established at various times during the H-mode periods.

3.3 Termination of high β_{POL} H-modes

The radiation in the ELM-free H phase remains relatively low (30-40% of the input power) and there is no sign of strong impurity influx so it is unlikely that radiative collapse is responsible for termination of the high β_{POL} phase. An analysis of MHD activity Hender et al, 1992) shows that there is no correlation between the n = 1, m = 1 internal kink and the rapid decline in β_{POL}, which appears to be an edge stability problem associated with a large ELM.

The two candidate mechanisms for the β_{POL} collapse are interaction with the ICRF antennae protection tiles and an edge ballooning instability. Evidence for the first comes from the thermographic observations of the antennae showing localised heating of the midplane edge carbon protection tiles as the plasma edge is brought closer to the antennae tiles by the automatic feedback control system which seeks to maintain the coupling resistance (see traces in fig. 5(a)). The antenna heating tends to be localised because the outer plasma boundary curvature exceeds that of the antennae. It is possible that this increased interaction leads to the large ELM with the radiated power fraction rising rapidly

to 100%, however no strong carbon influx due to the heating is seen prior to the ELM.

The second possibility of edge ballooning instability is shown in high n ballooning analysis of the edge plasma (Challis et al, 1993; Hender et al, 1992). As indicated in section 5, the edge of the high β_{POL} discharges have pressure and current density profiles which indicate access to the second stable ballooning regime. The edge density and pressure gradients become very large ($dn_e/dr \sim 2\ 10^{20} m^{-4}$) however, and as the edge current density evolves, just prior to the onset of the giant ELM the present gradients are calculated to be marginally stable to high n ballooning over the outer 0.1-0.15m of the plasma. There is some evidence from high frequency density fluctuations to support this. These fluctuations are measured with the multichannel reflectometer (Prentice et al, 1990), which shows increased high frequency (~ 100 kHz) fluctuations within 10 cm of the plasma edge ($n_e \leq 2\ 10^{19}\ m^{-3}$). As the time of the large ELM approaches, the fluctuation power spectrum broadens, with fluctuation levels at 100 kHz increasing by 2 orders of magnitude relative to those at 50 kHz. This phenomenon seems to precede many ELMs in JET plasmas (Ali-Arshad et al, 1992) and hence cannot be regarded as unique evidence of a ballooning limit and so we believe that a definitive choice between the two possible explanations for β_{POL} collapse requires further experiments.

4. HOT ION (HI) H-MODES

The highest fusion yields from deuterium plasmas in JET ($\approx 4.3 \times 10^{16}$ neutrons/second) have been achieved in the hot-ion (HI) H-mode regime (Thompson et al, 1993). The hot-ion regime is characterised by a relatively high ion temperature ($T_i(0)$ = 15-25keV) and $T_i(0) \geq 1.5T_e(0)$. These conditions are obtained by applying intense NBI heating to a low-moderate density ($n_e < 2 \times 10^{19} m^{-3}$) target plasma. It has also been possible to couple small amounts of ICRF power to these discharges. This has increased the fusion reactivity but lowered the Q_{DD}. Incremental NBI heating on the other hand, shows that Q_{DD} is approximately **proportional** to P_{nbi} (Thompson et al, 1993). HI H-modes are produced in plasmas with a magnetic X-point configuration with either a single or double null. Preparation of the interior surfaces of the tokamak vacuum vessel has proved to be important. Helium glow discharge cleaning or beryllium evaporation both of which result in low wall impurity retention and low particle recycling during the discharges are essential pre-requisites to achieving the highest performance,

including the very good confinement, which can be obtained in this regime. Peak enhancement factors (H_G^{DIA}) up to ~ 4 have been observed.

The duration of the H-mode phase in hot-ion plasmas is generally < 1.7 seconds which is slightly longer than τ_E but only a couple of percent of τ_R. The density rises throughout, and reaches values of $n_e(o) \approx 5 \times 10^{19} m^{-3}$ at the termination. Electron temperature sawteeth are generally stabilised for periods in excess of

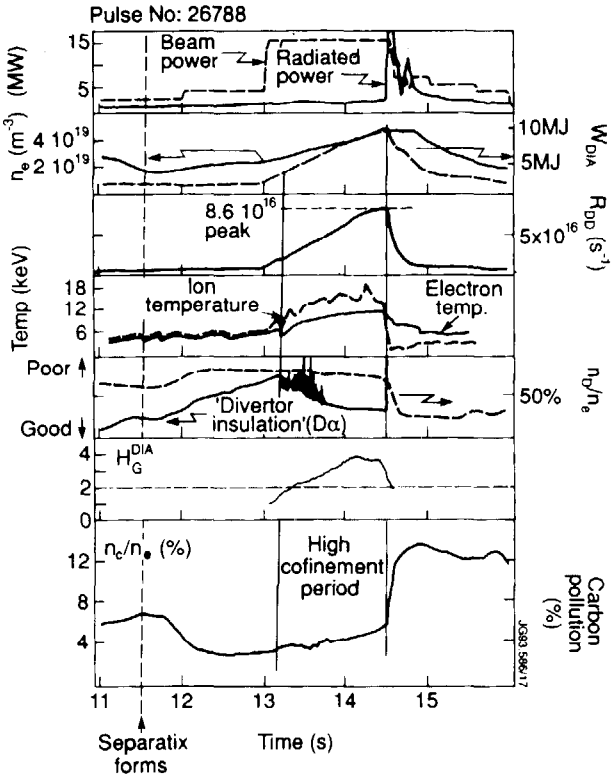

Fig. 7. Time development of a Hot Ion (HI) H-mode which reaches confinement enhancement relative to Goldston L-mode (H_G^{DIA}) ~ 4 before rapid collapse. (I_p = 3.1MA; B_T = 3.1T; q95 ~ 3.6; ion ∇B drift away from target).

1 second. Fig. 7 shows the time evolution of a HI H-mode plasma including the H factor. The plasma stored energy and neutron yield do not reach a steady state, but are still rising when a termination event sequence occurs which results in a reduction in both confinement and fusion yield.

4.1 Termination of the high performance phase in the HI H-modes

The high performance phase of HI H-modes terminates in a variety of ways. Some exhibit an abrupt loss of neutron yield and confinement while for others a rollover occurs with a timescale of 100's of ms. Abrupt terminations commonly have an ELM and sometimes an electron temperature sawtooth associated with them. Within a few milliseconds of the termination, a carbon bloom is observed

(presumably from the X-point target tiles) which prevents the recovery of the high performance state.

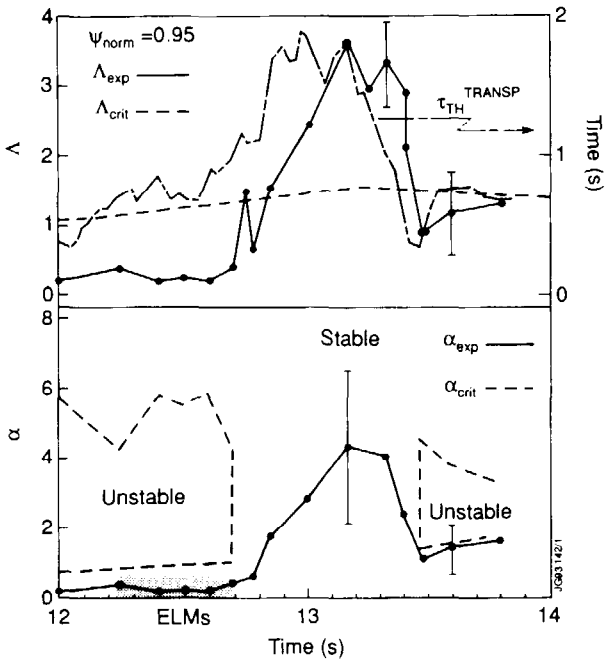

Fig. 8. Time evolution of confinement time from the plasma diamagnetic energy, normalised plasma pressure gradient measured near the plasma boundary (α_{exp}) and calculated stability boundary to ideal ballooning modes at the same radius (α_{ideal}) for one of the best performance HI H-modes (3.1MA/2.8T; HGDIA reaches H_G^{DIA} ~4.2 at 13.3 secs).

The pressure gradient at the edge of HI H-mode plasmas is typically very large and is calculated to give rise to a significant bootstrap current density. Under these circumstances, there is a region at the plasma periphery which is unconditionally stable to ideal ballooning modes (Balet et al, 1993b). The normalised edge pressure gradient achieved in one of the highest performance HI H-modes is plotted as a function of time in fig. 8 together with the region which is calculated to be unstable to ideal ballooning modes. At the end of the period of ELMs there is no region of instability for the plasma periphery and there is a coincident increase in global plasma energy confinement and local pressure gradient. However, no causal link between the disappearance of the unstable region and the improvement in confinement has been demonstrated. The unstable region returns coincidentally with the termination event.

Theoretical analyses of the termination of the high performance phase have investigated Ideal and Resistive Ballooning and Internal Kink mechanisms but have so far proved inconclusive. The origin of the ELM termination may be the result of edge gradients unstable to resistive ballooning (Huysmans et al, 1992) but not all discharges show marginal stability in this case. The Internal Kink analysis (Huysmans, 1993) shows that the mode structure for n = 1 is very sensitive to the edge current density gradient (j') and has an enhanced amplitude

at the plasma boundary for high values of j'_{edge} such as are known to exist in the HI H-modes. The Internal Kink also extends to large radii at high β_{POL}. It is clear that this is a candidate mechanism for the fast (sawtooth plus ELM) termination, but predictions have not been made for the relative instability of different HI H-modes in the dataset.

4.2 Effect of Toroidal field on HI H-mode performance and termination

The effect of the toroidal field strength on the behaviour and performance of HI H-modes has been investigated. Experiments have been performed with toroidal fields in the range B_T = 1.9–3.3T using NBI heating in the range of 14-16MW. The peak values of the plasma stored energy measured by the diamagnetic loop are seen when averaged over the data set to increase significantly ($\sim B_T^{0.5\text{-}0.7}$) as a function of toroidal field strength. The peak confinement enhancement factor, which is typically obtained earlier than the peak stored energy, shows a milder dependence on the field however ($B_T^{0.3\text{-}0.4}$). An indication of the resolution of these findings is given by considering the time histories of 3 HI H-modes with differing toroidal fields (but otherwise similar parameters) as shown in fig. 9. The plasma stored energy in the 3 discharges initially follows a similarly time evolution until 0.5-0.6 seconds. The stored energy then begins to limit in the lower field (1.8 and 2.2T) plasmas, and the confinement enhancement declines before the termination event around 1.25s.

Fig. 10 shows the maximum values of normalised β ($\beta_N = \beta_T a B_T / I_P$ with β_T in %, I_p in MA, a in m and B_T in Tesla) for the 3MA 1991/92 HI H-mode dataset plotted as a function of toroidal field strength. The best values of normalised β achieved so far do not appear to depend strongly on the toroidal field strength raising the possibility that these discharges are encountering a β limit especially at low field. However, since the characteristics of the termination of the high confinement phase vary throughout the dataset and the causes of the termination are still unclear, it is not possible to ascribe the achieved values of normalised β to a common cause or to demonstrate a β limit unambiguously.

Higher values of normalised β have been obtained in NBI heated JET plasmas at low current (I_p = 1.5-2MA) and low toroidal field ($B_T \leq 1.4$T) (Stork et al, 1992). In these discharges, values of β up to 6% have been achieved at a normalised β of 3.3.

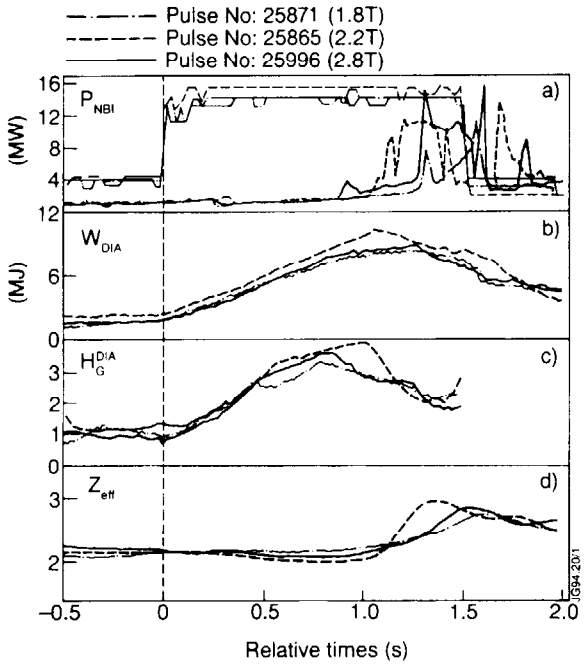

Fig. 9. Time evolution of three Double Null X-point plasmas attaining the HI H-mode. The three plasmas have very similar beam powers (trace (a)) and differ mainly in the toroidal field. Note the progressively earlier limitation in stored energy and decreasing limiting value of H_G^{DIA} as the Toroidal field is reduced.

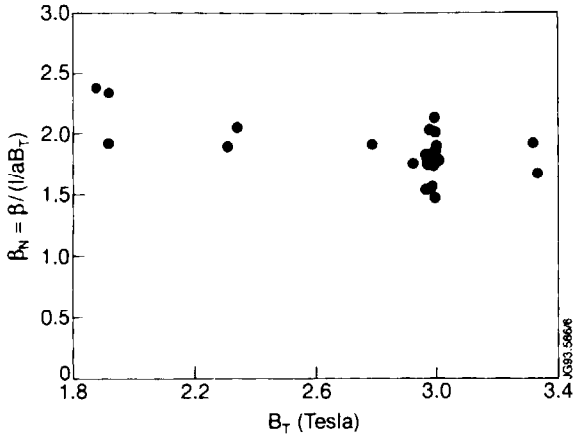

Fig. 10. Peak normalised β ($\beta_N = \beta_T a B_T / I_p$ with β_T in %, I_p in MA, a in m and B_T in Tesla) versus toroidal field strength for Hot-Ion H-modes.

4.3 Fusion performance in JET plasmas

Fig. 11 shows the values of the fusion triple product ($n_D(0)T_i(0)\tau_E$) obtained in the best JET plasmas and curves of equivalent thermal Q_{DT} (ratio of the fusion yield to the loss power) for comparison assuming a deuterium to tritium ratio of unity. This is equivalent to defining Q with respect to input power in steady state. The high performance domain is dominated by HI H-modes. Some PEP H-mode plasmas also appear on the diagram but since the assumed density and temperature profiles in the calculation of equivalent Q_{DT} are broad (parabolic) the comparison with the peaked profile PEP H-mode data is not strictly valid. However, values for the fusion triple product of up to $7.5\pm0.5 \times 10^{20} m^{-3} keV.s$ have been achieved with a central ion temperature around 10keV in this regime.

Consideration of fig. 11 reveals that the best of the HI H-modes establish plasma conditions which are outside of the previously defined 'Hot Ion' region of the

$n_D(0)T_i(0)\tau_E$ plot (Bickerton et al, 1987). They are moving towards equilibration of the ion and electron temperatures and hence into a more optimum regime for the route to an ignited plasma. The principal reason for this is that the ion energy confinement is significantly better than the electron energy confinement in the centre of these plasmas (see eg: Thompson et al, 1992).

The HI H-mode was chosen as the discharge for performing the world's first experiment with a D-T plasma (JET Team 1992). The total fusion power producedin this experiment was 1.7MW for an input NBI power of 14.3MW, a ratio of fusion power to input power of approximately 0.12.

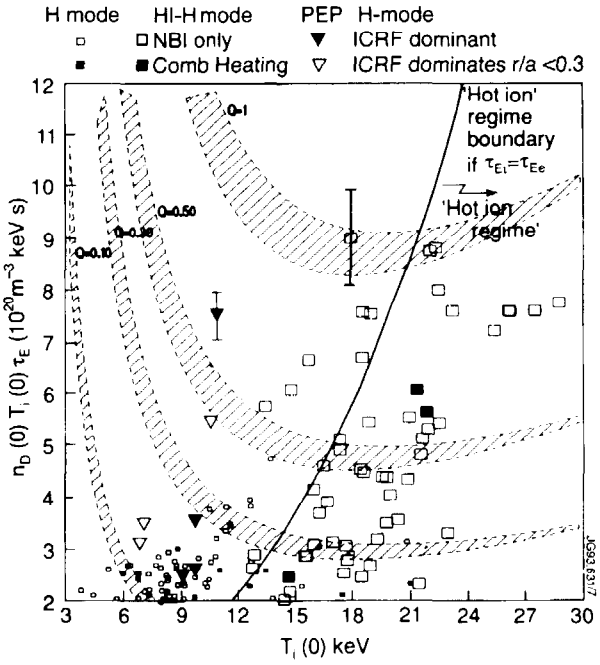

Fig. 11. Triple fusion product ($n_D(o)$. $T_i(o)\cdot \tau_E$) plotted against central ion temperature ($T_i(o)$) for the best JET plasmas with > 10MW additional heating. The line marked 'hot ion regime boundary' indicates the relationship defined in Bickerton et al (1987).

The bars on the highest point represent the approximate accuracy of the quantities and applicable to all points.

Note that the 'Q' curves refer to equivalent 50:50 D-T plasmas in steady state and are only valid for broad parabolic profiles of density and temperature. Their comparison with the PEP H-modes is thus not strictly valid.

5. A UNIFIED VH REGIME IN JET

A regime of plasma performance known as the VH mode regime has been identified in the DIII-D tokamak (Jackson et al, 1991). This regime is characterised

by thermal confinement which reaches levels up to 2.4 times the JET/DIII-D ELM free H-mode scaling and was achieved following the initial boronisation of the vessel. It has been postulated that this regime is also being observed in the JET H-modes with elevated energy confinement (Balet et al, 1993; Greenfield et al, 1993). We must therefore address the question of whether or not the JET H-mode discharges with *globally* elevated energy confinement (the high β_{POL} and HI H-modes) are in reality two aspects of a unified regime.

The answer to this question would appear to be yes. Apart from the similar global VH level of confinement, the two regimes both have a large bootstrap current at the plasma edge and this allows access to the regime of second stability against ballooning modes. An analysis by Deliyanakis et al (1993) shows that up to 30% of the plasma volume is in the second stable region in the well developed ELM-free phase. Both regimes have edge pressure profiles which expand into the region of second stability in the s,α plane but it is as yet unclear as to the mechanism which is propelling this enhancement.

The plasmas also seem to limit at $\beta_N \sim 2$ ($\pm$ 10%) which is further suggestive of a unified regime.

The identification of a VH regime in JET plasmas encompasses a wide variety of plasma scenarios. This fact gives information about the relative importance of various physics issues in the achievement of VH conditions. Since ICRF heating is used to obtain the 1MA high β_{POL} VH regime and NBI heating the 3MA HI VH regime, it is clear that VH modes can be obtained with power transfer to either electrons or ions. In addition the high β_{POL} plasmas have very little plasma rotation (Thomas et al 1993), with toroidal velocities more than an order of magnitude slower than the HI H-modes. This implies that significant rotation 'spin-up' is not necessary before the VH regime can be accessed, a finding in marked contrast to studies in DIII-D (Burrell et al, 1992; Greenfield et al, 1993). The plasma shaping used in the JET VH regime plasmas provides insufficient triangularity to give access to the second stable regime without the presence of the bootstrap current, again in contrast to the situation in DIII-D (Jackson et al, 1992; Taylor et al, 1993). This is a possible reason why the normalised β_N achieved in the JET VH plasmas is lower than the best DIII-D values as the regime clearly has to develop a second stable region as the discharge develops. Examination of the JET HI and high β_{POL} plasmas shows that the dependence of confinement enhancement (H) is not a strong function of triangularity (δ) (fig.-12).

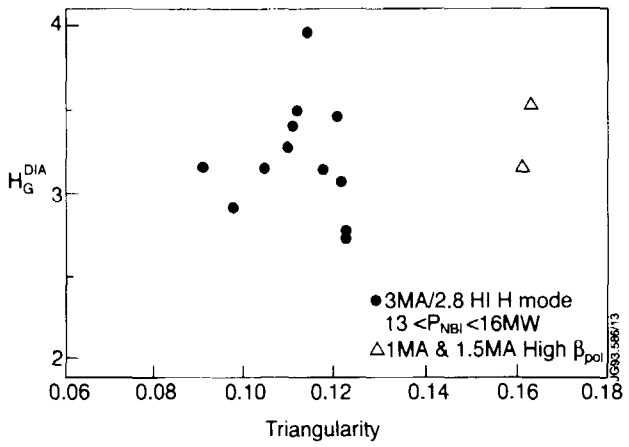

Fig. 12. Confinement enhancement (H_G^{DIA}) plotted against triangularity (δ) for a sub-group of the HI H-modes and typical high β_{POL} H-modes.

In order to establish an *operational* philosophy for accessing the VH regime in JET, we have examined the 3MA H-mode database to find the dependence of confinement enhancement relative to L mode (H_G^{DIA}) on various discharge parameters. A similar analysis for the low current (1MA) high β_{POL} VH modes obtained with ICRF heating has not been done as the parameter variation in that dataset is not very wide. The results for the 3MA H/VH modes are shown in fig. 13(a)-(e).

Fig. 13(a) shows that if the dataset is divided merely into Hot Ion H-modes ($T_i > 1.5T_e$ and $T_i > 10$keV) and others that the strong tendency is for the VH plasmas to be dominantly Hot Ion. Fig. 13(b) shows that the poor Hot Ion H`modes are all from the earlier (1988 and 1989) JET experimental campaigns. Inthis period the X-point of the discharge was usually near or on the vessel's carbon X-point tiles. From 1990 onwards, the Single Null (SNX) and Double Null (DNX) discharges had X-points which were well inside the vessel (at least 5cm 'inside' the location of the X-point tiles).

This has clearly brought benefits for the HI H-modes but the improvement in the 'normal' H-modes is less clear (fig. 13(c)). The improvement with time is also indicative of improved vessel conditioning (beryllium evaporation) and the movement of the X-point has helped to reduce recycling and insulate the plasma.

Fig. 13(d) shows that (again with the exception of the earlier Hot Ion shots) a higher toroidal field is statistically beneficial in accessing the VH regime.

Fig. 13(e) emphasises the importance of a pure plasma (low Z_{eff}) and indicates that the earlier Hot Ion shots suffered from pollution.

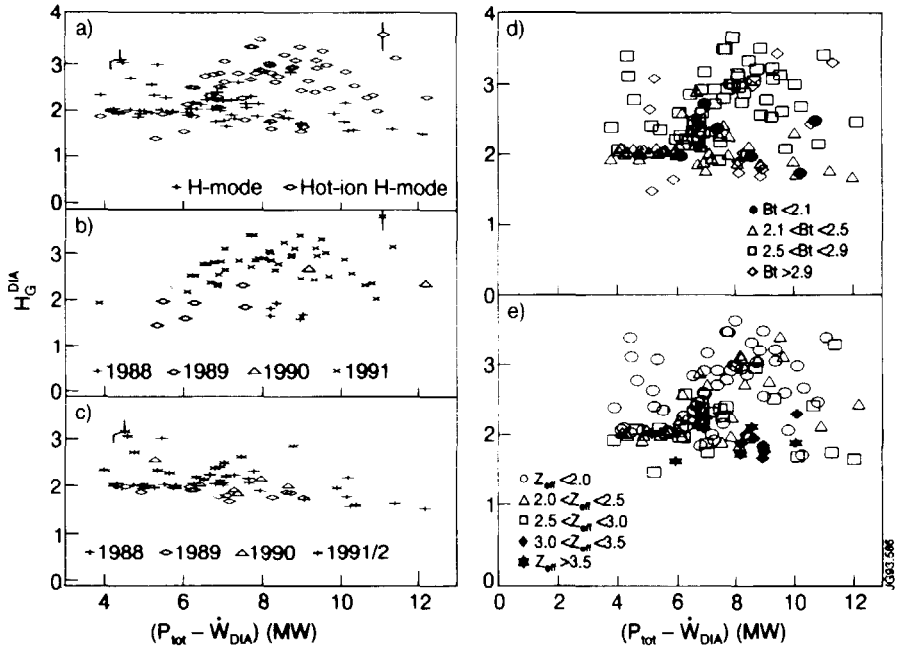

Fig. 13. An examination of the JET 3MA H-modes with steady NBI heating (additional power constant for ≥ 0.6secs).

The enhancement factor (H_G^{DIA}) is plotted against loss power and the dataset is grouped according to:

a) Hot Ion ($T_i > 1.5T_e$; $T_i > 10$keV) and non Hot Ion

b) Year of experiment for Hot Ion H-modes

c) Year of experiment for normal H-modes

d) Toroidal field value

e) Effective ion charge of the plasma (Z_{eff}) during the steady power phase.

Parameters which are *not* seen to be important in accessing the VH regime are number of nulls (SNX and DNX discharge are both represented at high values of H_G^{DIA}) and the direction of the ion ∇B drift (∇B drift into and out of the X-point are both represented at high values of H_G^{DIA}).

5.1 Discussion of access to the VH regime

For the 3MA H-mode dataset, the important parameters for accessing the VH regime all have a clear effect on the generation of a high edge bootstrap current. The low recycling of the HI H-modes (performed without gas puff) and the improved shielding against impurities given by a large X-point to tile distance

both reduce the edge collisionality and enhance the bootstrap current. Low recycling and the low power and particle transport out of the centre of the Hot Ion plasmas tend to increase ∇n and ∇T at plasma edge and further enhance the bootstrap current. It is also true that the edge values of ∇T_i and ∇T_e are higher at high toroidal fields. Although the exact reason for this is not clear it also leads to further bootstrap enhancement. These conditions, when taken in totality, seem to be capable of generating sufficient bootstrap current to give access to the second stable regime.

In the 1MA high β_{POL} plasma, strong gas puffing is used at the outer midplane (~ 1.5 10^{21} atoms sec $^{-1}$) and the low recycling conditions are violated. It is possible, though not proven, that triangularity may be a key to the second stability access in these discharges. They are certainly the highest triangularity plasmas in the JET dataset. It is also possible that the very high edge q(q_{95} ~ 13) may play an important role in keeping the plasma profiles far from the first stability boundary until the conditions have developed for access to the second stable region. A high value of q also results in a long connection length in the divertor region which helps to isolate the plasma from returning neutrals and impurities.

6. CONCLUSIONS

The JET device has successfully produced plasmas where β_{POL} reaches ~ 2; either globally, in discharges with 70% bootstrap fraction; or locally, in the Pellet Enhanced Plasma (PEP) H-modes. Three H-mode regimes have been established on JET where the global confinement enhancement reaches values of ≥ 3 but these H-mode plasmas (the high I_b/I_p H-mode; PEP H-mode and Hot Ion (HI) H-mode), remain transient on a resistive diffusion timescale.

The confinement enhancement in the PEP H-mode is predominantly in the central 25% volume of the plasma and may be associated with the negative shear region in the core. The enhancement in the high I_b/I_p (high β_{POL}) and HI H-modes is seen to be approximately uniform throughout the plasma.

The high β_{POL} and HI H-modes both feature large edge bootstrap current and, for the period of the elevated confinement, these give the plasma edge access to the 'second stability regime' which is unconditionally stable against ideal ballooning modes. The mechanism which *causes* the plasma pressure to increase

subsequently so that the measured profiles exist in the second stable region has not been identified.

The access to second stability indicates that the high β_{POL} and HI H-modes are two aspects of a unified VH mode regime for JET plasmas. That this is the case indicates that the VH regime can either be obtained with electron heating (ICRF) or ion heating (NBI) and that high plasma toroidal rotation is not necessary before the VH regime is accessed.

The operational parameters for accessing the VH regime have been investigated. For the high power (HI H-mode) shots low recycling; an X-point well separated from the vessel; a high toroidal field; a low value of Z_{eff} and a central hot ion plasma appear to be important operational parameters. All these conditions are seen to be helpful in establishing high edge gradients and hence a high edge bootstrap current. For the low power (high β_{POL} H-mode) shots which can be obtained with strong gas puffing, it is possible that the higher triangularity in these discharges (bringing them closer to the unconditional second stable access) plays an important role. Also the high edge safety factor ($q_{95} \sim 13$) is associated with high values of q in the separatrix region which may serve to isolate the plasma from returning neutrals and impurities.

The VH regime plasmas appear to limit at $2 \Psi \beta_N \Psi 2.4$ but it is difficult to determine unambiguously a β-limit because of the variable character of the termination of the regime. Analyses suggest that ideal ballooning instability at the plasma edge might be responsible for the high β_{POL} H-mode collapse. Other analyses show that it is possible that the internal ($n = 1$) kink has a significant amplitude across the plasma cross section when high current gradients exist at the plasma edge. This may explain the fast global collapses seen in the high power VH mode discharge.

The PEP H-mode also has access to the second stable region but in this case it is the core of the plasma which is affected. Analyses show that the PEP H phase may be terminated by a variety of reasons including ballooning instability as the current profile evolves to close down the access to second stability, and $n = 1$ or $n = 3$ resistive kinks which are de-stabilised in a sequence which varies according to the initial axial safety factor.

The VH regime in JET has already produced the best central fusion products and fusion performance in its high power Hot Ion manifestation. Plasmas with $n_D(o)T_i(o)\tau_E$ values of $9 \pm 1\ 10^{20}m^{-3}keVs$ have been produced and these plasmas are developing along a route which is optimum relative to the minima in the contours of equivalent Q_{DT}. The 1994 campaign in JET will attempt to push this regime to higher performance using combined heating with NBI (22MW) and ICRF (24MW) and will attempt to extend the duration of the regime using the improved performance of the JET Pumped Divertor.

ACKNOWLEDGEMENTS

The principal author would like to acknowledge the contribution of the whole JET Team to this work. In particular it is a pleasure to acknowledge significant contributions and useful discussions with my colleagues Drs B Alper, B Balet, C D Challis, H J de Blank, H P L de Esch, N Delyanakis, C Gormezano, G Huysmans, J Jacquinot, T T C Jones, D P O'Brien, J O'Rourke, P Smeulders, P M Stubberfield, P R Thomas, K Thomsen, E Thompson, F Tibone and B J D Tubbing. The contribution of collaborators from AEA Culham (L Appel, C Gimblett, J Hastie and T C Hender) and from General Atomics (C Greenfield) is also gratefully acknowledged.

REFERENCES

Ali-Arshad S et al, 1992, *Europhys Conf Abstracts 16C(I)*, 227.
Balet B et al, 1992, *Plasma Phys and Contr Fusion* 34, 3.
Balet B et al, 1993, *Proc of Varenna Workshop on Local Transport Studies in Plasmas*, in press.
Balet B et al, 1993b submitted for publication in *Nuclear Fusion*.
Bhatnagar V et al, 1991, *Europhys Conf Abstracts* 15(C)I, 373.
Bickerton R J and the JET Team, 1987, *Plasma Phys and Contr Fusion* 29, 1219.
Bures M et al, 1993, *Europhys Conf Abstracts* 17C(I), 171.
Burrell K H et al, 1992, *Plasma Phys and Contr Fusion* 34, 1859.
Campbell D J et al, 1993, these proceedings.
Challis C D et al, 1992, *Nuclear Fusion* 32, 2217.
Challis C D et al, 1993, *Nuclear Fusion* 33, 1097.
de Esch H P L et al, 1990, *Europhys Conf Abstracts* 15C(I), 189.
Deliyanakis N et al, 1993, *Europhys Conf Abstracts* 17C(I), 155.

Greenfield C M et al, 1993, submitted for publication in *Plasma Phys and Contr Fus.*
Hender T C et al, 1992, *Europhys Conf Abstracts* 16C(I), 335.
Huysmans G T et al, 1992, *Europhys Conf Abstracts* 16C(I), 247.
Huysmans G T, 1993, private communication.
Jackson G L et al, 1991, *Phys Rev Letts* 67, 3098.
Jackson G L et al, 1992, *Phys Fluids* B4, 2181.
Jones T T C et al, 1992, *Europhys Conf Abstracts* 16(C)I, 3.
The JET Team, 1992, *Nuclear Fusion* 32, 187.
Prentice R et al, 1990, *Europhys Conf Abstracts* 14B (IV), 1500.
Rebut P H, Lallia P P and Watkins M L, 1988, *Plasma Phys and Contr Fus Research* (Proc 12th Int Conf) (IAEA Vienna), Vol 2, 191.
Rebut P H, 1990, *Fusion Eng. and Design* 14, 171.
Schissel D P et al, 1991, *Nucl Fusion* 31, 73.
Smeulders P et al, 1993, submitted for publication in *Nuclear Fusion.*
Stork D et al, 1990, *Journal Nucl Matls* 176 & 177, 409.
Stork D et al, 1991, *Europhys Conf Abstracts* 15(C)I, 357.
Stork D et al, 1992, *Europhys Conf Abstracts* 16C(I), 339.
Stubberfield P M et al, 1992, *Europhys Conf Abstracts* 16C(I), 63.
Tanga A et al, 1987, *Nucl Fusion* 27, 1877.
Taylor T S et al, 1993, *Plasma Phys and Contr Nucl Fus Research* (Proc 14th Int Conf) (IAEA Vienna), Vol 1, 167.
Thomas P R and the JET Team, 1993, to be published in *Phys Fluids B.*
Thompson E, Stork D, de Esch H P L and the JET Team, 1993, *Phys Fluids* B5, 246.
Thomsen K et al, 1993, these proceedings.
Tubbing B J D et al, 1991, *Nucl Fusion* 31, 839.

Appendix I

THE JET TEAM

JET Joint Undertaking, Abingdon, Oxon, OX14 3EA, U.K.

J.M. Adams[1], Y. Agarici[3], B. Alper, H. Altmann, P. Andrew, S.Ali-Arshad, W. Bailey, B. Balet, P. Barabaschi, Y. Baranov[8], P. Barker, R. Barnsley[2], M. Baronian, D.V. Bartlett, A.C. Bell, G. Benali, P. Bertoldi, E. Bertolini, V. Bhatnagar, A.J. Bickley, H. Bindslev, K. Blackler, D. Bond, T. Bonicelli, S.J. Booth, K. Borras[13], G. Bosia, M. Botman, P. Boucquey, M. Brandon, P. Breger, H. Brelen, W.J. Brewerton, T. Brown, M. Brusati, T. Budd, M. Bures, P. Burton, T. Businaro, P. Butcher, H. Buttgereit, C. Caldwell-Nichols, D.J. Campbell, D. Campling, P. Card, G. Celentano, C.D. Challis, A. Cherubini, D. Chiron, J. Christiansen, P. Chuilon, R. Claesen, S. Clement, J.P. Coad, I.H. Coffey[6], A. Colton[14], M. Comiskey[4], M. Cooke, S. Cooper, J.G. Cordey, G. Corrigan, S. Corti, A.E. Costley, G. Cottrell, M. Cox[7], P. Crawley, O. Da Costa, N. Davies, S.J. Davies[7], J.J. Davis, H. de Esch, E. Deksnis, N. Deliyanakis, G.B. Denne-Hinnov, G. Deschamps, W.J. Dickson[19], A. Dines, S.L. Dmitrenko, J. Dobbing, N. Dolgetta, S.E. Dorling, P.G. Doyle, H. Duquenoy, A. Edwards, J. Ehrenberg, A. Ekedahl, T. Elevant[11], S.K. Erents[7], L.G. Eriksson, H. Falter, G. Fishpool, J. Freiling[15], C. Froger, P. Froissard, K. Fullard, M. Gadeberg, A. Galetsas, L. Galbiati, M. Garribba, P. Gaze, R. Giannella, A. Gibson, R.D. Gill, A. Girard, A. Gondhalekar, D. Goodall[7], C. Gormezano, N.A. Gottardi, C. Gowers, R. Haange, A. Haigh, C.J. Hancock, P.J. Harbour, N.C. Hawkes[7], N.P. Hawkes[1], P. Haynes[7], J.L. Hemmerich, T. Hender[7], J. Hoekzema, L. Horton, J. How, P.J. Howarth[5], M. Huart, T.P. Hughes[4], F. Hurd, B. Ingram, M. Irving, J. Jacquinot, H. Jaeckel, J.F. Jaeger, G. Janeschitz, O.N. Jarvis, F. Jensen, M. Johnson, E.M. Jones, L.P.D.F. Jones, T.T.C. Jones, J-F. Junger, F. Junique, A. Kaye, B.E. Keen, M. Keilhacker, W. Kerner, N.G. Kidd, R. Konig, A. Korotkov[8], P. Kupschus, R. Lässer, J.R. Last, L. Lauro-Taroni, K. Lawson[7], M. Lennholm, J. Lingertat[13], R.N. Litunovski, A. Loarte, P. Lomas, M. Loughlin, C. Lowry, A.C. Maas[15], B. Macklin, C.F. Maggi[16], G. Magyar, V. Marchese, F. Marcus, J. Mart, D. Martin, E. Martin, T. Martin, P. Massmann, G. Matthews, H. McBryan, P. Meriguet, S.F. Mills, R. Monk, P. Morgan, H. Morsi, G. Murphy, F. Nave[21], G. Newbert, M. Newman, P. Nielsen, M. Nilsen[17], P. Noll, W. Obert, D. O'Brien, M. O'Mullane[18], E. Oord, J. O'Rourke, R. Ostrom, M. Ottaviani, S. Papastergiou, V.V. Parail, B. Patel, A. Peacock, N. Peacock[7], R.J.M. Pearce, C. Perry, M.A. Pick, J. Plancoulaine, J-P. Poffé, F. Porcelli, L. Porte[19], R. Prentice, S. Puppin, G. Radford[9], T. Raimondi, M.C. Ramos de Andrade, M. Rapisarda[22], R. Reichle, S. Richards, E. Righi, F. Rimini, A. Rolfe, R. Rookes[12], R.T. Ross, L. Rossi, R. Russ, G. Sadler, G. Saibene, J.L. Salanave, M. Salisbury[12], G. Sanazzaro, A. Santagiustina, R. Sartori, C. Sborchia, P. Schild, M. Schmid, B. Schunke, S.M. Scott, A. Sibley, R. Simonini, A.C.C. Sips, P. Smeulders, R. Smith, F. Söldner, M. Stamp, P. Stangeby[20], D.F. Start, C.A. Steed, D. Stork, P.E. Stott, P. Stubberfield, D. Summers, H. Summers[19], W. Suverkropp, L. Svensson, T. Szabo, M. Tabellini, A. Tanga, A. Taroni, C. Terella, A. Tesini, P.R. Thomas, E. Thompson, K. Thomsen, P. Trevalion, B. Tubbing, H. van der Beken, G. Vayakis, G. Vlases, M. von Hellermann, T. Wade, C. Walker, D. Ward, M.L. Watkins, M.J. Watson, S. Weber[10], J. Wesson, T.J. Wijnands, D. Wilson, T. Winkel, R. Wolf, C. Woodward, M. Wykes, I.D. Young, L. Zannelli, W. Zwingmann.

PERMANENT ADDRESSES

1. UKAEA, Harwell, Didcot, Oxon, UK.
2. University of Leicester, Leicester, UK.
3. CEA, Cadarache, France.
4. University of Essex, Colchester, UK.
5. University of Birmingham, Birmingham, UK.
6. Queens University, Belfast, UK.
7. UKAEA Culham Laboratory, Abingdon, Oxon, UK.
8. A.F. Ioffe Institute, St. Petersburg, Russia.
9. Institute of Mathematics, University of Oxford, UK.
10. Freien Universität, Berlin, Germany.
11. Royal Institute of Technology, Stockholm, Sweden.
12. Imperial College, University of London, UK.
13. Max Planck Institut für Plasmaphysik, Garching, Germany.
14. Risø National Laboratory, Denmark.
15. FOM Instituut voor Plasmafysica, Nieuwegein, The Netherlands.
16. Dipartimento di Fisica, University of Milan, Milano, Italy.
17. General Atomics, San Diego, USA.
18. University College, Cork, Ireland.
19. University of Strathclyde, 107 Rottenrow, Glasgow, UK.
20. Institute for Aerospace Studies, University of Toronto, Canada.
21. LNETI, Savacem, Portugal.
22. ENEA, Frascati, Italy.

At 1st July, 1993